Organic LETTERS

Letter

pubs.acs.org/OrgLett

Wollamides: Antimycobacterial Cyclic Hexapeptides from an Australian Soil *Streptomyces*

Zeinab G. Khalil,[†] Angela A. Salim,[†] Ernest Lacey,[‡] Antje Blumenthal,*[,§,∥] and Robert J. Capon*[,†]

[†]Institute for Molecular Bioscience, The University of Queensland, St. Lucia, QLD 4072, Australia

[‡]Microbial Screening Technologies, Smithfield, NSW 2164, Australia

[§]The University of Queensland Diamantina Institute, The University of Queensland, Brisbane, QLD 4102, Australia

[∥]Australian Infectious Diseases Research Centre, The University of Queensland, Brisbane, QLD 4072, Australia

Supporting Information

ABSTRACT: A soil *Streptomyces* nov. sp. (MST-115088) isolated from semiarid terrain near Wollogorang Station, Queensland, returned two known and two new examples of a rare class of cyclic hexapeptide, desotamides A and B (**1** and **2**) and E and F (**3** and **4**), respectively, together with two new D-Orn homologues, wollamides A and B (**5** and **6**). Structures were assigned by detailed spectroscopic and C_3 Marfey's analysis. The desotamides/wollamides exhibit growth inhibitory activity against Gram-positive bacteria (IC_{50} 0.6−7 μM) and are noncytotoxic to mammalian cells (IC_{50} >30 μM). The wollamides exhibit antimycobacterial activity (IC_{50} 2.8 and 3.1 μM), including reduction in the intracellular mycobacterial survival in murine bone marrow-derived macrophages.

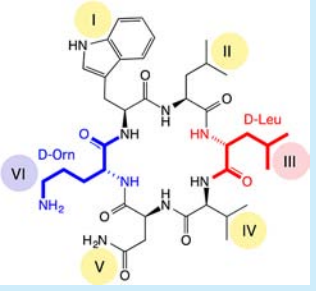

Mycobacterium tuberculosis (TB) is one of the most enduring therapeutic hurdles in global health. Front line antitubercular treatment, which is limited to protracted high dose combination therapy employing 60 year old vintage antibiotics of variable efficacy (i.e., isoniazid, pyrazinamide, ethambutol, rifampicin, and streptomycin), must combat the growing threat posed by multi (MDR-TB), extensively (XDR-TB), and totally (TDR-TB) drug-resistant TB infections.[1] Meeting this challenge demands an innovative and ongoing commitment to the discovery of new antitubercular drugs. Recently, the "re-discovery" of known classes of natural products has proven to be an effective strategy for developing new approaches to treating tuberculosis. For example, a 2012 investigation of the *Streptomyces* metabolite pyridomycin revealed an antitubercular molecular target (InhA) in common with isoniazid, prompting its description as "nature's isoniazid".[2] Significantly, as the most frequently encountered isoniazid-resistant clinical isolates of TB are susceptible to pyridomycin, this reveals that pyridomycin engages with a new druggable InhA binding pocket. Such knowledge can inform future efforts at discovering new antitubercular agents. Similarly, a 2014 investigation of the *Streptomyces* antibiotic spectinomycin saw the development of the semisynthetic spectinamides with improved antitubercular activity, capable of evading the Rv1258c efflux pump up-regulated in many MDR TB strains.[3]

These "re-discovery" events affirm the potential of known *Streptomyces* metabolites as privileged antibacterial scaffolds, capable of informing the development of next generation antitubercular drugs.

During an investigation into *Streptomyces* from Australian soils we detected an elegant example of nature's capacity for "re-discovery" in a *Streptomyces* nov. sp. (MST-115088) isolated from semiarid soil near Wollogorang Station, Queensland, Australia. Although taxonomic sequencing revealed >99% sequence homology with eight *Streptomyces* strains belonging to six different species (Supporting Information), chemotaxonomic considerations confirmed that MST-115088 differed from all known *Streptomyces* strains. HPLC-DAD-ESIMS analysis of the MeOH extract revealed a secondary metabolite profile attributed to neutral and basic tryptophan-containing peptides (Supporting Information). Subsequent solvent partitioning, gel chromatography, and reversed-phase HPLC fractionation returned the rare cyclic hexapeptides desotamide (**1**)[4] and desotamide B (**2**),[5] together with two new homologues, desotamides E (**3**) and F (**4**), and the new D-Orn substitution homologues, wollamides A (**5**) and B (**6**) (Figure 1). Structures were assigned to **1**−**6** on the basis of detailed spectroscopic and C_3 Marfey's analysis.

Desotamide (**1**) was first described in 1997 from a soil *Streptomyces* collected near DeSota Falls, GA, as a cometabolite with the bicyclic peptide salinamide and the nucleoside herbicidin A.[4] Desotamide B (**2**) was only recently described in 2014 from a deep-sea *Streptomyces scopuliridus* (SCSIO ZJ46) collected in the South China Sea, as a cometabolite with desotamide and desotamides C and D.[5] In these studies, the structure elucidation of **1** and **2** was achieved by detailed spectroscopic analysis (and in the case of **1** total synthesis[4]). To confirm the isolation of **1** and **2** from MST-115088 we employed detailed spectroscopic analysis plus C_3 Marfey's and MS analyses (Supporting Information).

Received: August 20, 2014
Published: September 17, 2014

dx.doi.org/10.1021/ol502472c | *Org. Lett.* 2014, 16, 5120−5123

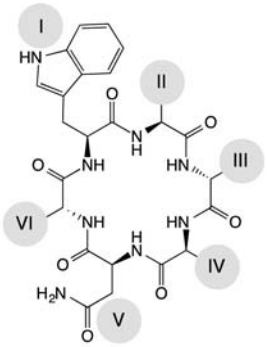

	I	II	III	IV	V	VI
(1)	L-Trp	L-Leu	D-Leu	L-*allo*-Ile	L-Asn	Gly
(2)	L-Trp	L-Leu	D-Leu	L-Val	L-Asn	Gly
(3)	L-Trp	L-Leu	D-Val	L-*allo*-Ile	L-Asn	Gly
(4)	L-Trp	L-Leu	D-*allo*-Ile	L-*allo*-Ile	L-Asn	Gly
(5)	L-Trp	L-Leu	D-Leu	L-*allo*-Ile	L-Asn	D-Orn
(6)	L-Trp	L-Leu	D-Leu	L-Val	L-Asn	D-Orn

Figure 1. *Streptomyces* nov. sp. (MST-115088) metabolites **1**–**6**.

HRESI(+)MS analysis of **3** revealed a molecular formula ($C_{34}H_{50}N_8O_7$, Δmmu +2.9) consistent with a homologue ($-CH_2$) of **1**. By employing C_3 Marfey's methodology (Figure 2), which features an optimized C_3 reversed-phase HPLC-

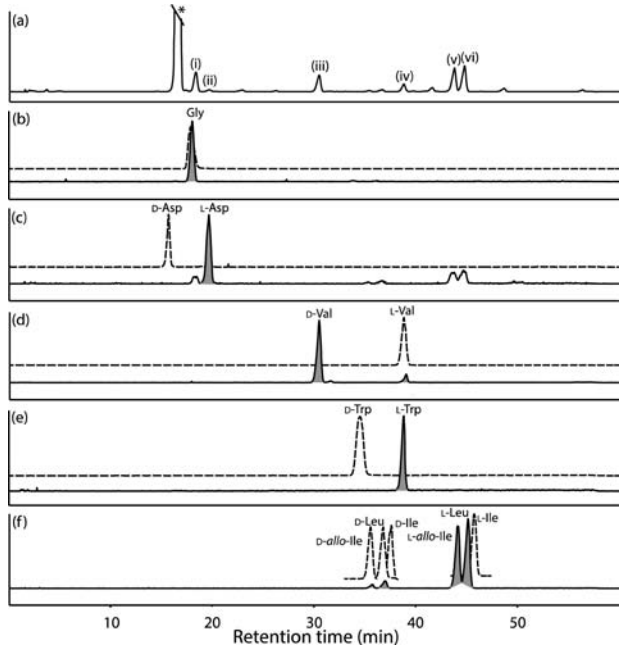

Figure 2. C_3 Marfey's analysis of desotamide E (**3**). i–vi indicate constituent amino acids as D-FDAA derivatives. * indicates residual Marfey's reagent.

DAD-ESI(+)MS analysis of the D-FDAA derivatized acid hydrolysate of **3**, comparing the 360 nm extract from the HPLC-DAD chromatogram (Figure 2a) and selected single ion extracts (SIE) from the HPLC-ESI(+)MS chromatograms (Figure 2b–f, solid traces) with authentic standards (Figure 2b–f, dashed traces), we successfully identified all six amino acid residues in **3**. Of note, while this analysis detected L-Asp, based on the molecular formula for **3** this was taken as evidence for L-Asn. Consistent with this interpretation, under the acid hydrolysis conditions used for the C_3 Marfey's analysis, we noted that authentic L-Asn underwent quantitative hydrolysis to L-Asp. Pursuing this issue further, we detected L-Asn in a C_3 Marfey's analysis of **3** subjected to acid hydrolysis in the presence of thioglycolic acid (an additive known to suppress L-Asn hydrolysis)[6,7] (Supporting Information). Significantly, the C_3 Marfey's methodology outlined above successfully resolved all Leu, *allo*-Ile, and Ile isomers (Figure 2) and readily confirmed the presence of L-Leu and L-*allo*-Ile residues in **3**. Diagnostic 2D NMR (DMSO-d_6) correlations (Figure 3)

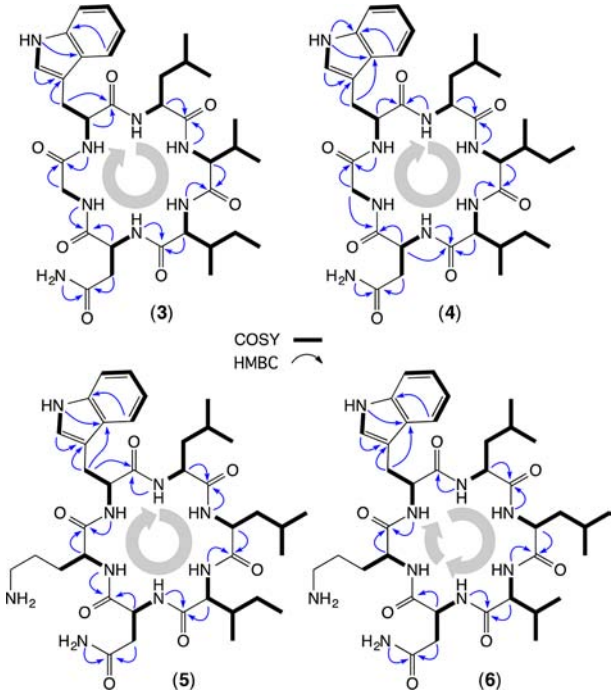

Figure 3. Diagnostic 2D NMR (DMSO-d_6) correlations for **3**–**6**. Note: The bold arrow(s) highlights connectivity sequences.

established the connectivity sequence from L-Trp to L-Leu to D-Val to L-*allo*-Ile to L-Asn to Gly, which was further confirmed by MS fragmentations (Figure 4). Collectively, these observations confirmed the structure for desotamide E (**3**) as indicated (as a D-Leu to D-Val substitution homologue of **1**).

HRESI(+)MS analysis of **4** revealed a molecular formula ($C_{35}H_{52}N_8O_7$, Δmmu +1.6) isomeric with **1**, with the amino acid residues identified by C_3 Marfey's analysis (Supporting Information) being consistent with a D-Leu to D-*allo*-Ile substitution homologue. Supportive of this hypothesis, diagnostic 2D NMR (DMSO-d_6) correlations (Figure 3) established the connectivity sequences L-Trp to L-Leu to D-*allo*-Ile (L-*allo*-Ile) to L-*allo*-Ile (D-*allo*-Ile) to L-Asn to Gly, while MS fragmentations (Figure 4) established a contiguous but nonspecified sequence of the isomeric amino acids L-Leu, D-*allo*-Ile, and L-*allo*-Ile, bearing a pendant L-Asn residue. Collectively, these observations permitted assignment of the structure for desotamide F (**4**) as indicated, less the D-*allo*-Ile and L-*allo*-Ile relative regiochemistry.

HRESI(+)MS analysis of **5** revealed a molecular formula ($C_{38}H_{59}N_9O_7$, Δmmu +0.1) consistent with a Gly to Orn substitution of **1**, with the amino acid residues identified by C_3 Marfey's analysis (Supporting Information) attributing this substitution to a D-Orn. Diagnostic 2D NMR (DMSO-d_6) correlations (Figure 3) established the connectivity sequence L-Trp to L-Leu (D-Leu) to D-Leu (L-Leu) to L-*allo*-Ile to L-Asn to D-Orn, while MS fragmentations (Figure 4) established the

dx.doi.org/10.1021/ol502472c | *Org. Lett.* 2014, 16, 5120–5123

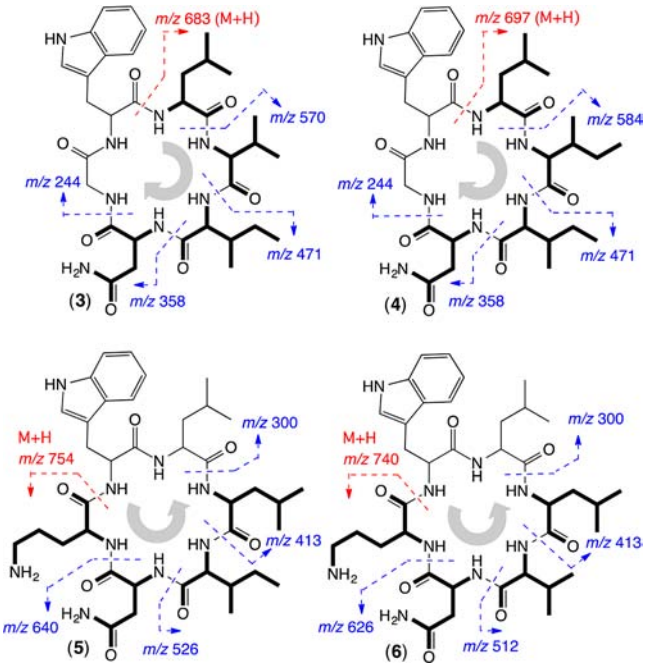

Figure 4. Diagnostic MS fragmentations for **3** − **6**. Note: The bold arrow highlights connectivity sequences.

sequence D-Orn to L-Asn to L-*allo*-Ile (D-Leu or L-Leu) to D-Leu (L-*allo*-Ile or L-Leu). Of note, whereas **3** and **4** exhibited common MS fragmentation pathways initiated by cleavage of the amide bond between L-Trp and residue II (tracking clockwise, Figure 4), in the case of **5** the MS fragmentation sequence was initiated by cleavage of the amide bond between L-Trp and D-Orn (tracking anticlockwise, Figure 4). Collectively, these observations permitted assignment of the structure for wollamide A (**5**) as indicated, less the D-Leu and L-Leu relative regiochemistry.

HRESI(+)MS analysis of **6** revealed a molecular formula ($C_{37}H_{57}N_9O_7$, Δmmu −1.9) consistent with a homologue ($-CH_2$) of **5**, with the amino acid residues identified by C_3 Marfey's analysis (Supporting Information) further refining this to an L-*allo*-Leu to L-Val substitution. Diagnostic 2D NMR (DMSO-d_6) correlations (Figure 3) established the connectivity sequence L-Leu (D-Leu) to D-Leu (L-Leu) to L-Val to L-Asn, and from D-Orn to L-Trp, while MS fragmentations (Figure 4) established the sequence D-Orn to L-Asn to L-Val to D-Leu (L-Leu). Of note, the MS fragmentation pathway for **6** was consistent with that for **5** and differed from that observed for **3** and **4**. Collectively, these observations permitted assignment of the structure for wollamide B (**6**) as indicated, less the D-Leu and L-Leu relative regiochemistry.

To complete the structure elucidation of **4**−**6** we applied biosynthetic considerations to propose a common stereochemical motif in which the presence of a D-amino acid at residue III in **1**−**3** is extended to **4**−**6** (i.e., D-*allo*-Leu for **4** and D-Leu for **5** and **6**). It is interesting to note conservation across **1**−**6** with respect to the amino acid residues I, II, and V and the limited diversity across residues III and IV (D-Leu, D/L-*allo*-Ile and D/L-Val) and residue VI (Gly and D-Orn).

The cyclic hexapeptides **1**−**6** exhibited significant growth inhibitory activity against the Gram-positive bacteria *Bacillus subtilis* (ATCC 6633 and ATCC 6051) (IC_{50} 2−10 μM) with **4** and **6** also exhibiting activity against *Staphylococcus aureus* (ATCC 9144 and ATCC 25923) (IC_{50} 0.6−7 μM) (Table 1).

Table 1. Antibacterial Activity (IC_{50} μM) for 1−6

	Staphylococcus aureus		*Bacillus subtilis*	
	ATCC 25923	ATCC 9144	ATCC 6051	ATCC 6633
1			5.2	10.1
2			4.3	4.0
3			5.2	3.5
4	6.8	5.5	1.0	1.2
5			1.8	2.0
6	0.6	0.9	1.9	2.2

For blanks cells IC_{50} > 30 μM.

By contrast, **1**−**6** displayed no growth inhibitory activity (IC_{50} > 30 μM) against the Gram-negative bacteria *Escherichia coli* (ATCC 11775) and *Pseudomonas aeruginosa* (ATCC 10145), the fungus *Candida albicans* (ATCC 90028), or human colon (SW620) and lung (NCI) cancer cell lines (Supporting Information). This antibiotic/cytotoxicity profile encouraged us to examine the growth inhibitory activity of **1**−**6** against *M. bovis*, Bacille Calmette Guerin.

Significantly, the basic wollamides **5** and **6** inhibited growth of *M. bovis*, BCG in liquid culture (IC_{50} 2.8 and 3.1 μM, respectively) and exhibited bactericidal activity against BCG (Figures 5a−c), whereas the neutral desotamides **1**−**4** exhibited no BCG growth inhibitory or bactericidal activity. Of particular

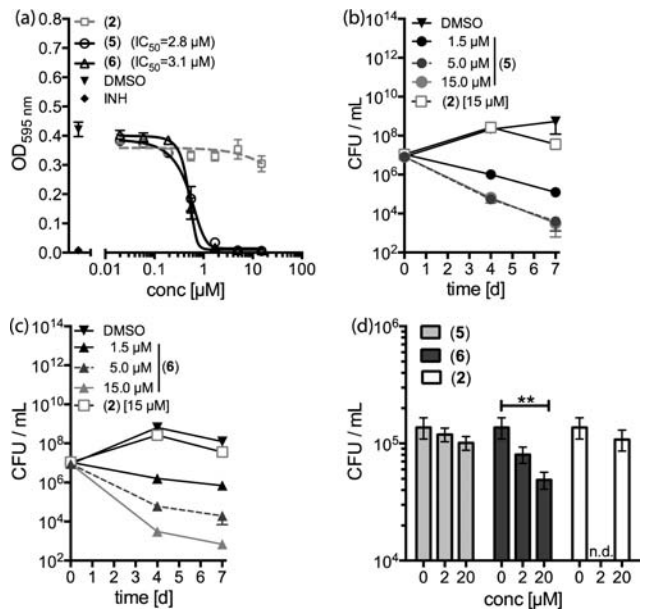

Figure 5. Antimycobacterial screening of **2**, **5**, and **6**. (a) Optical density (OD) determination of *M. bovis* BCG cultures after 7 days growth in the presence or absence of **2**, **5**, and **6** (0.02−15 μM). DMSO and isoniazid (INH; 20 μg/mL) served as negative and positive controls, respectively. Data are means ± SEM of six independent BCG cultures. (b, c) Colony-forming units (CFU) of *M. bovis* (BCG) in in vitro cultures exposed to **2**, **5**, and **6** at the indicated concentrations for four and 7 days. Data points are means ± SEM of three to six independent BCG cultures. (d) Primary mouse bone marrow-derived macrophages were infected with BCG and cultured in the presence or absence of **2**, **5**, and **6** or DMSO. CFU in cell lysates were determined on day 6 post-infection. Data are means ± SEM of six replicate wells obtained in two independent experiments. Each treated group was compared to DMSO treatment using One-Way ANOVA, Dunnett's correction. $^{**}p < 0.01$. n.d. = not determined.

dx.doi.org/10.1021/ol502472c | *Org. Lett.* 2014, 16, 5120−5123

note, addition of **6** (2 and 20 μM) to infected macrophage, the major host cell for mycobacteria, significantly reduced the number of viable intracellular *M. bovis* BCG 6 days after infection (41 and 64% respectively) (Figure 5d), with microscopic observation of the macrophage cultures revealing no cytotoxic effects.

The low mammalian cytotoxicity and selective antibacterial and antimycobacterial profiles demonstrated by **5** and **6** are particularly encouraging and offer a perspective on how microbes can repurpose an existing biosynthetic infrastructure. By replacing the only achiral amino acid (Gly) in the desotamide cyclic hexapeptide scaffold with a basic D-amino acid (D-Orn), the antibacterial profile of the secondary metabolite complex produced by *Streptomyces* nov. sp. (MST-115088) has been expanded to include mycobacteria—one of the most challenging bacterial pathogens. The implications of this modification on the tertiary structure of these cyclic peptides, and its correlation to activating antimycobacterial properties, represent a promising new area for enquiry. Chemical synthesis and/or precursor directed biosynthesis could deliver new wollamide analogues that would inform structure—activity relationship investigations, defining the mechanism of action, and potentially delivering new (improved) antitubercular drugs.

■ ASSOCIATED CONTENT

Supporting Information

Full experimental details, NMR spectra, tabulated 2D NMR data, and bioassay results. This material is available free of charge via the Internet at http://pubs.acs.org.

■ AUTHOR INFORMATION

Corresponding Authors

*E-mail: a.blumenthal@uq.edu.au.
*E-mail: r.capon@uq.edu.au.

Notes

The authors declare no competing financial interest.

■ ACKNOWLEDGMENTS

We acknowledge the assistance of D. Vuong, A. Crombie, and A. E. Lacey (MST) for assistance with genetic sequencing, fermentation, and metabolite purification. We thank S. Bates and R. Robey (NCE, NIH) for providing the SW620 cell line, A. Jones (UQ) for acquiring the MS/MS data, A. Piggott (UQ) for helpful discussions, and T. Nguyen (UQ) for assistance in the BCG macrophage infection assay. Z.G.K. acknowledges the provision of a UQ International Postgraduate Scholarship. A.B. acknowledges support by a research fellowship by the International Balzan Foundation. This research was funded in part by the Institute for Molecular Bioscience, The University of Queensland, and the Australian Research Council (LP120100088).

■ REFERENCES

(1) Garcia, A.; Bocanegra-Garcia, V.; Palma-Nicolas, J. P.; Rivera, G. *Eur. J. Med. Chem.* **2012**, *49*, 1−23.
(2) Hartkoorn, R. C.; Sala, C.; Neres, J.; Pojer, F.; Magnet, S.; Mukherjee, R.; Uplekar, S.; Boy-Roettger, S.; Altmann, K.; Cole, S. T. *EMBO Mol. Med.* **2012**, *4*, 1032−1042.
(3) Lee, R. E.; Hurdle, J. G.; Liu, J.; Bruhn, D. F.; Matt, T.; Scherman, M. S.; Vaddady, P. K.; Zheng, Z.; Qi, J.; Akbergenov, R.; Das, S.; Madhura, D. B.; Rathi, C.; Trivedi, A.; Villellas, C.; Lee, R. B.; Rakesh; Waidyarachchi, S. L.; Sun, D.; McNeil, M. R.; Ainsa, J. A.; Boshoff, H. I.; Gonzalez-Juarrero, M.; Meibohm, B.; Boettger, E. C.; Lenaerts, A. J. *Nat. Med.* **2014**, *20*, 152−158.
(4) Miao, S.; Anstee, M. R.; LaMarco, K.; Matthew, J.; Huang, L. H. T.; Brasseur, M. M. *J. Nat. Prod.* **1997**, *60*, 858−861.
(5) Song, Y.; Li, Q.; Liu, X.; Chen, Y.; Zhang, Y.; Sun, A.; Zhang, W.; Zhang, J.; Ju, J. *J. Nat. Prod.* **2014**, *77*, 1937−1941.
(6) Gehrke, C. W.; Takeda, H. *J. Chromatogr.* **1973**, *76*, 77−89.
(7) Catak, S.; Monard, G.; Aviyente, V.; Ruiz-Lopez, M. F. *J. Phys. Chem. A* **2009**, *113*, 1111−1120.